materials

MDPI

Article

Experimental Investigation of Charring and Axial Deformation of Korean Larch Glued-Laminated Timber Columns Under Long-Duration Standard Fire Exposure

Huirak Ahn, Jaehong An and Yunjeong Choi *

Construction Test & Assessment Center, Korea Institute of Civil Engineering and Building Technology, Ilsanseo-gu, Goyang-si 10223, Gyeonggi-Do, Republic of Korea; huirakahn@kict.re.kr (H.A.); rehong@kict.re.kr (J.A.)
* Correspondence: yjchoi@kict.re.kr

Highlights

- Mean charring depth increased from 39.9 to 102.6 mm over 60–180 min of fire exposure.
- At 180 min, charring depths were similar at load ratios of 0.8 and 1.0 (106.5–107.3 mm).
- Final axial displacements differed by 19.01 mm between load ratios of 0.8 and 1.0.
- Both axial load and residual cross-sectional area should be considered in fire response assessments.
- This study provides 180-min fire test data for large-section Korean larch GLT columns.

Abstract

The fire response of large-section glued-laminated timber (GLT) columns depends on both progressive charring and sustained axial loading. This study investigated Korean larch GLT columns with a 500 mm × 500 mm cross section and a height of 3000 mm under four-sided standard fire exposure. Five non-load-bearing specimens were tested for 60–180 min, while load-bearing tests were conducted for 180 min at prescribed load ratios of 0.8, 1.0, and 1.2; the last case was excluded from quantitative comparison because its target load was not maintained. Mean charring depth increased from 39.9 mm at 60 min to 102.6 mm at 180 min, while the corresponding time-averaged charring rate decreased from 0.67 to 0.57 mm/min. A linear regression of mean charring depth against exposure duration yielded $R^2 = 0.993$ over the 60–180 min range. After 180 min, mean charring depths were 106.5 and 107.3 mm at load ratios of 0.8 and 1.0, respectively, whereas final axial displacements were −0.66 and 18.35 mm. The equivalent residual cross-sectional area ratios calculated from the measured mean charring depths were 32.9% and 32.6%, respectively. These results indicate that similar geometric section losses can be accompanied by substantially different axial deformation responses, underscoring the importance of considering both charring and applied load when evaluating GLT columns subjected to prolonged standard fire exposure.

Keywords: glued-laminated timber; Korean larch; fire resistance; charring behavior; axial displacement; residual cross-sectional area

Check for updates

Academic Editors: Dorota Dukarska and Jakub Kawalerczyk

Received: 29 October 2026
Revised: 18 November 2026
Accepted: 23 November 2026
Published: 25 November 2026

Copyright: © 2026 by the authors. Licensee MDPI, Basel, Switzerland. This article is an open access article distributed under the terms and conditions of the Creative Commons Attribution (CC BY) license.

1. Introduction

In recent years, reducing carbon emissions and promoting the use of sustainable structural materials have become important challenges in the construction industry, leading to the increasing application of timber as a primary structural material in mid- and high-rise buildings. Life cycle assessment studies of structural systems have reported that engineered

timber-based structures may offer advantages in reducing carbon emissions compared with reinforced concrete and steel structures. These environmental benefits have become one of the major factors driving the structural application of large-section engineered timber [1,2]. In particular, glued-laminated timber (GLT) is an engineered wood product manufactured by bonding graded timber laminations with their grain directions parallel to one another. Owing to its improved material uniformity and structural performance, GLT has been widely used as a primary load-bearing structural material for columns and beams in mid- and high-rise timber buildings.

As the application of timber structural members expands, ensuring structural safety under fire exposure has become an essential consideration in structural design. Although wood is a combustible material, exposure to fire causes thermal decomposition at its surface, resulting in the formation of a char layer that delays heat transfer to the underlying wood. Consequently, while the outer cross-sectional region is progressively consumed during fire exposure, a residual cross-section capable of maintaining structural resistance for a certain period remains beneath the char layer. Charring behavior is influenced by various factors, including wood species, density, moisture content, cross-sectional dimensions, and fire exposure conditions. Accordingly, charring depth and charring rate are commonly used as key parameters for evaluating the residual cross-section and load-bearing capacity of timber structural members exposed to fire [3–5].

Based on the fire behavior of wood, structural fire design methods for timber members generally evaluate residual load-bearing capacity by considering the reduction in cross-sectional dimensions caused by fire exposure. Eurocode 5 provides a method for determining the effective cross-section by accounting for both the char layer and the region in which mechanical properties have deteriorated due to elevated temperatures [6]. The reduced cross-section method has been widely adopted as a representative approach for evaluating the structural resistance of timber members exposed to fire [7]. However, the appropriate thickness of the zero-strength layer may depend on several factors, including cross-sectional geometry, stress conditions, applied load level, and fire exposure duration. Previous studies have indicated that, particularly for compression members such as columns, a simplified reduction in cross-sectional dimensions may not adequately represent their actual structural behavior under fire exposure [7–9]. Previous studies have also investigated the fire performance of timber building elements through combined experimental and numerical approaches. Ferreira et al. [10] examined the fire resistance and thermal behavior of traditional timber-based walls under standard fire exposure, while Couto et al. [11] investigated the fire behavior of perforated wooden slabs using experimental and numerical methods. These studies highlight the importance of experimental validation and thermal analysis in evaluating the fire performance of timber components. However, further experimental investigations are required to characterize the axial deformation and residual cross-sectional characteristics of large-section GLT columns under prolonged fire exposure.

These considerations are particularly important for GLT columns. In actual buildings, GLT columns must continue to sustain axial loads during fire exposure. As charring progresses, the effective cross-sectional area and second moment of area progressively decrease. Consequently, the compressive stress acting on the residual cross-section may increase, while the stiffness and stability of the column deteriorate, potentially increasing its susceptibility to axial deformation and buckling. Therefore, the fire resistance of GLT columns may depend not only on material degradation characteristics, such as charring rate, but also on the interaction between the reduced residual cross-section and the applied load. Previous fire resistance tests on GLT and heavy timber columns have demonstrated that load level and slenderness ratio can influence fire resistance performance [12]. More recent experimental studies on loaded GLT columns have shown that deformation may

continue to increase during the cooling phase following fire exposure, potentially leading to structural failure [13]. Furthermore, a comprehensive analysis of existing fire test data and design models has highlighted the need for additional experimental evidence and further validation of design methods to improve the prediction of the structural fire behavior of laminated timber compression members [9].

Fire exposure duration is another important parameter in evaluating the performance of GLT columns. Structural fire design methods often simplify the charring behavior of wood by assuming a constant charring rate. However, the thickness and thermal resistance of the char layer change with increasing fire exposure duration, potentially resulting in time-dependent variations in charring behavior [3–5]. Under prolonged fire exposure, the progressive reduction in cross-sectional area becomes more pronounced, while the remaining cross-section must continue to sustain the applied load. Therefore, the relationship between charring behavior and structural response becomes increasingly important. Charring characteristics evaluated at specific fire resistance periods or under relatively short fire exposure durations may not sufficiently describe the structural behavior of large-section GLT columns subjected to prolonged fire exposure. Accordingly, it is necessary to evaluate both the progression of charring with increasing fire exposure duration and the associated deformation behavior under different loading conditions.

Material characteristics associated with wood species also play an important role in the fire behavior of GLT. Li et al. [14] conducted standard fire resistance tests on glulam columns manufactured from six different wood species and investigated the relationships between wood density, charring characteristics, and heat penetration. Their findings indicated that wood species with relatively higher densities may exhibit lower charring rates and slower heat penetration. These results demonstrate that the fire behavior of GLT can vary depending on the material characteristics of the wood species, emphasizing the need for experimental verification using locally available timber species intended for structural applications. In Korea, Korean larch is one of the major timber species used in the manufacture of structural GLT. To facilitate its application as a large-section structural member in mid- and high-rise timber buildings, further experimental data on charring characteristics and structural behavior under prolonged fire exposure are required.

Experimental investigations have also been conducted on the fire behavior of Korean larch GLT columns. Choi et al. [15] performed load-bearing and non-load-bearing fire resistance tests on Korean larch GLT columns with a cross-section of 300 mm × 300 mm under standard fire exposure conditions. Their study evaluated charring characteristics at fire exposure durations ranging from 30 to 120 min under non-load-bearing conditions and investigated charring and deformation behavior under different load ratios in load-bearing tests. The study provided valuable experimental data on the charring characteristics and loading effects of Korean larch GLT columns. It also reported that the influence of applied load level on mean charring depth was relatively limited within the investigated loading conditions [15].

Nevertheless, experimental studies simultaneously evaluating the time-dependent progression of charring and load-dependent structural responses of large-section GLT columns under prolonged standard fire exposure remain limited. In particular, whereas previous investigations on Korean larch GLT columns focused on cross-sectional dimensions of 300 mm × 300 mm and fire exposure durations of up to 120 min [15], experimental verification of the charring characteristics and structural behavior of larger cross-sectional members exposed to standard fire conditions for up to 3 h remains insufficient. Furthermore, comparisons between load-bearing and non-load-bearing test results under identical prolonged fire exposure conditions are required to distinguish the effects of applied load on charring behavior from the structural deformation associated with different loading levels

in progressively reduced residual cross-sections. Recent investigations of GLT columns exposed to real fires have also emphasized the importance of the relationship between residual cross-sectional characteristics and post-fire axial load-bearing capacity [16]. In addition, studies involving fire scenarios different from standard fire exposure have demonstrated that the charring behavior of GLT may vary depending on fire conditions [17]. Therefore, evaluating the progression of charring and reduction in residual cross-sectional area under prolonged standard fire exposure, together with the associated load-dependent axial deformation behavior, is important for extending conventional charring-rate-based assessments toward a more comprehensive evaluation of structural fire behavior.

To address these research gaps, the present study conducted standard fire resistance tests on large-section GLT columns manufactured from Korean larch, with cross-sectional dimensions of 500 mm × 500 mm and a height of 3000 mm, for fire exposure durations of up to 180 min. To evaluate the influence of fire exposure duration on charring behavior, non-load-bearing fire resistance tests were performed at exposure durations of 60, 90, 120, 150, and 180 min. In addition, load-bearing fire resistance tests were conducted under different load ratios for 180 min to investigate charring characteristics and structural responses under prolonged fire exposure.

The scientific contribution of this study extends beyond the increased specimen dimensions and fire exposure duration. By examining the progression of charring and the corresponding reduction in geometric residual cross-sectional area, this study provides insight into the relationship between prolonged thermal exposure and cross-sectional loss in large-section GLT columns. Furthermore, comparisons between load-bearing and non-load-bearing specimens under identical 180 min fire exposure conditions allow the observed charring characteristics to be examined alongside the axial deformation responses of individual loaded specimens. In particular, the substantial difference in axial displacement observed between specimens with similar mean charring depths highlights the importance of considering structural deformation in addition to geometric cross-sectional reduction. Although the absence of replicate tests limits the generalization of these findings, the results provide experimental evidence relevant to understanding the coupled effects of charring-induced cross-sectional reduction and loading conditions on the structural fire response of large-section GLT columns.

2. Materials and Methods

2.1. Materials and GLT Column Specimens

In this study, a total of eight glued-laminated timber (GLT) column specimens were fabricated from domestically sourced Korean larch (*Larix kaempferi*) to investigate their charring characteristics and structural behavior under prolonged standard fire exposure. All specimens were manufactured with identical dimensions, consisting of a height of 3000 mm and a square cross-section of 500 mm × 500 mm. The geometry and dimensions of the GLT column specimens are shown in Figure 1.

The specimens were manufactured by laminating and bonding Korean larch timber laminations with their grain directions oriented parallel to the longitudinal axis of the columns. All specimens were fabricated as continuous members without mechanical joints along their height, thereby eliminating the influence of mechanical joints during fire testing.

The available manufacturing documentation confirmed the timber species, specimen dimensions, longitudinal grain orientation, and continuous member configuration. However, detailed records of the measured density, moisture content, conditioning procedure, individual lamination thickness, adhesive type, and strength-grading procedure were not identified in the available documentation. Accordingly, these characteristics could not be independently verified in the present study.

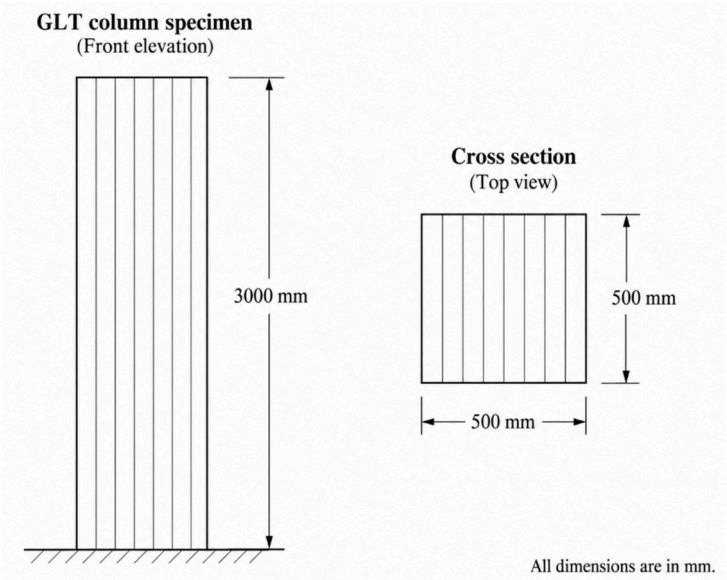


Figure 1. Geometry and dimensions of the GLT column specimen.

For the determination of the reference test load described in Section 2.3, the allowable compressive stress and modulus of elasticity corresponding to grade 10S-30B in KDS 41 50 10:2022 were adopted as reference design input parameters. These values were used for calculating the prescribed test loads and do not constitute independent verification that the tested specimens satisfied the requirements of grade 10S-30B.

The specimens were classified into load-bearing and non-load-bearing groups according to the test objectives. Different load ratios were applied to the load-bearing specimens to compare their charring behavior and axial deformation under prolonged fire exposure. For the non-load-bearing specimens, fire exposure durations of 60, 90, 120, 150, and 180 min were selected to investigate the charring characteristics as a function of fire exposure duration without external axial loading.

2.2. Fire Resistance Test Setup and Heating Conditions

The fire resistance tests of the GLT columns were conducted using a furnace designed for column testing. The specimens were installed vertically inside the furnace and subjected to simultaneous heating on all four sides. The furnace heating system consisted of nozzle-mix burners fueled by liquefied natural gas (LNG). For the load-bearing tests, an axial compressive load was applied to the specimens using a hydraulic loading system. The hydraulic actuator was located beneath the furnace and applied the compressive load to the bottom of the specimen. The loading system had a maximum loading capacity of 19 MN and a maximum compression stroke of 1000 mm. A schematic illustration of the fire resistance test setup and four-sided heating conditions for the GLT columns is presented in Figure 2. The fire resistance tests were conducted in accordance with the general requirements of KS F 2257-1 and the specific requirements for columns specified in KS F 2257-7 [18,19].

The furnace temperature was controlled in accordance with the standard time–temperature curve specified in KS F 2257-1. During the load-bearing fire resistance tests, the prescribed axial compressive load was maintained using the hydraulic loading system while the specimens were exposed to the standard fire. The standard time–temperature curve is expressed by Equation (1), as specified in KS F 2257-1 and ISO 834-1 [18,20].

$$T = 345 log_{10}(8t + 1) + 20 \quad (1)$$

where (T) represents the mean furnace temperature (°C), and (t) denotes the fire exposure duration (min). The standard time–temperature curve specified in KS F 2257 and applied in this study is presented in Figure 3.

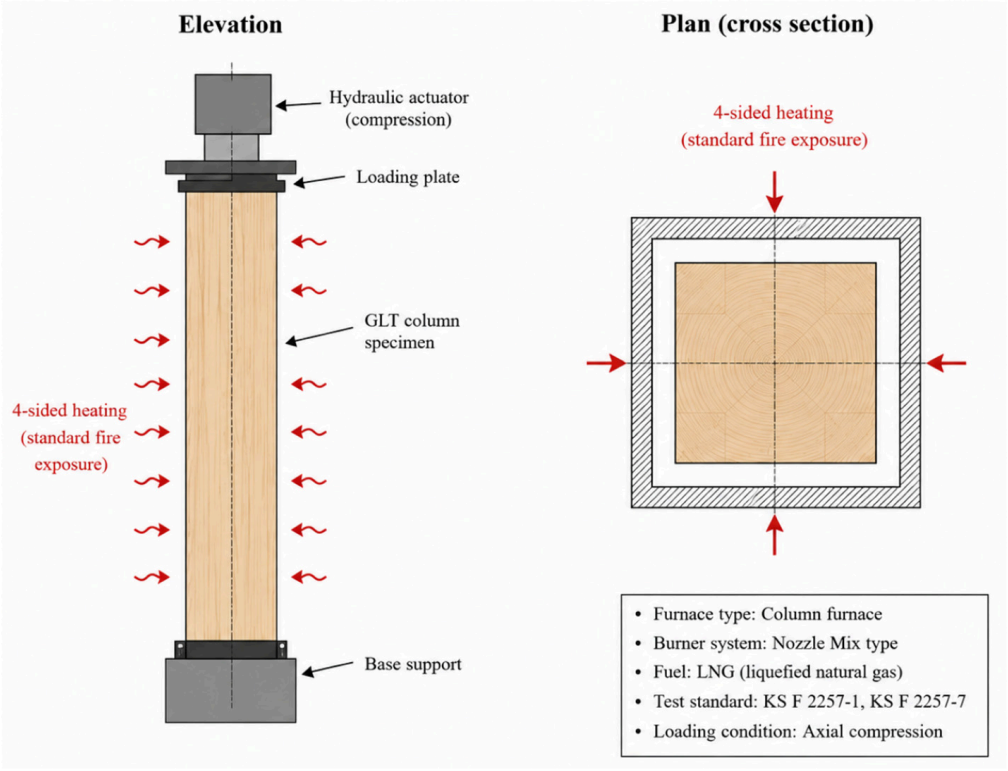


Figure 2. Schematic view of the fire test setup for the GLT column specimens.

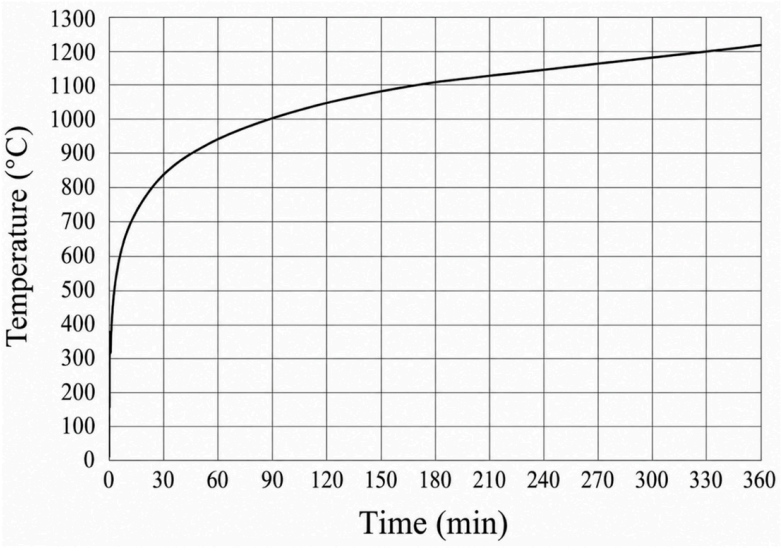


Figure 3. Standard time–temperature curve specified in KS F 2257-1 and ISO 834-1 [18,20].

During the fire resistance tests, the axial displacement of the specimens was continuously monitored as a function of fire exposure duration. The non-load-bearing fire resistance tests were conducted under the same standard fire exposure conditions as the load-bearing tests, but without applying an external axial load. Identical heating conditions were applied to both test groups, allowing the charring behavior of the GLT columns to be compared at the same fire exposure duration with and without axial loading.

2.3. Test Program and Loading Conditions

The primary test variables in this study were fire exposure duration and load ratio. For the non-load-bearing tests, fire resistance tests were conducted at exposure durations of 60, 90, 120, 150, and 180 min to evaluate the charring behavior of GLT columns as a function of fire exposure duration. The changes in charring depth and time-averaged charring rate with increasing fire exposure duration were subsequently analyzed.

The load-bearing tests were conducted under prolonged standard fire exposure for 180 min, with prescribed load ratios of 0.8, 1.0, and 1.2 to compare the structural behavior of GLT columns under different loading conditions. The reference test load was determined by considering the anticipated residual cross-section after 180 min of standard fire exposure and the reference allowable compressive stress of the column. A reference charring rate of 0.65 mm/min, adopted from Eurocode 5 [6], was used to estimate the charring depth, resulting in an initial value of 117 mm after 180 min. Two successive 10% allowances were additionally applied to account conservatively for potential corner effects and uncertainties associated with prolonged fire exposure. The resulting estimated charring depth was 141.57 mm, which was conservatively increased to 145 mm for specimen design. These additional allowances were assumptions adopted specifically for the present experimental design rather than requirements prescribed by Eurocode 5. Assuming a uniform charring depth of 145 mm on all four exposed faces, the anticipated residual cross-section was 210 mm × 210 mm, corresponding to a residual cross-sectional area of 44,100 mm^2.

For the calculation of the reference test load, a reference allowable compressive stress parallel to the grain of 7.5 MPa and a reference modulus of elasticity of 8000 MPa were adopted as design input parameters. These values correspond to the reference design values for symmetrically arranged mixed-grade glued-laminated timber of grade 10S-30B, as specified in Table 3.2-2 of KDS 41 50 10:2022 [21]. These material properties were used as reference design inputs for determining the test loads and were not intended to independently verify the actual strength grade of the specimens. For the reference-load calculation, the column stability factor was evaluated using the procedure specified in KDS 41 50 20:2022 [22]. The anticipated residual cross-section of 210 mm × 210 mm and the specimen height of 3000 mm were used for this calculation. Assuming an effective length factor of 1.0, the effective buckling length was taken as 3000 mm, corresponding to a slenderness ratio of approximately 14.29. Using a reference modulus of elasticity of 8000 MPa, an elastic modulus coefficient of variation of 0.10, and a glulam stability parameter of 0.9, the calculated column stability factor was approximately 0.933. The assumed effective length factor was adopted for the reference-load calculation and does not constitute independent verification of the actual rotational restraints provided by the test apparatus. With all other adjustment factors assumed to be 1.0, the adjusted allowable compressive stress was approximately 7.0 MPa. Accordingly, the reference test load was calculated to be approximately 309 kN by multiplying the adjusted allowable compressive stress by the anticipated residual cross-sectional area of 44,100 mm^2.

The load ratio was defined as the ratio of the applied axial compressive load to the reference test load, as expressed in Equation (2).

$$\eta = P/P_{ref} \tag{2}$$

where η denotes the load ratio, P represents the applied axial compressive load, and P_{ref} is the reference test load used to determine the load ratio. In this study, P_{ref} was set at 309 kN. Accordingly, target loads of 247, 309, and 370 kN were specified for specimens with prescribed load ratios of 0.8, 1.0, and 1.2, respectively. The dimensions and test conditions of all GLT column specimens are summarized in Table 1. In the specimen designations,

GL-C denotes a glued-laminated timber column, while L and NL represent load-bearing and non-load-bearing conditions, respectively.

Table 1. GLT column specimens and fire test conditions.

Specimen	Specimen Dimensions (mm)	Target Fire Exposure Duration (min)	Applied Load (kN)	Load Ratio	Fire Test Condition
GL-C-L-1.2-1	3000 × 500 × 500	180	370	1.2	Load-bearing
GL-C-L-1.0-1	3000 × 500 × 500	180	309	1.0	Load-bearing
GL-C-L-0.8-1	3000 × 500 × 500	180	247	0.8	Load-bearing
GL-C-NL-3.0h-1	3000 × 500 × 500	180	-	-	Non-load-bearing
GL-C-NL-2.5h-1	3000 × 500 × 500	150	-	-	Non-load-bearing
GL-C-NL-2.0h-1	3000 × 500 × 500	120	-	-	Non-load-bearing
GL-C-NL-1.5h-1	3000 × 500 × 500	90	-	-	Non-load-bearing
GL-C-NL-1.0h-1	3000 × 500 × 500	60	-	-	Non-load-bearing

During the load-bearing fire resistance tests, the axial displacement of the GLT columns was measured in accordance with the load-bearing capacity assessment procedures specified in KS F 2257-1. For specimens with a height of 3000 mm, the axial contraction and contraction-rate limits were calculated to be 30 mm and 9 mm/min, respectively [18]. The axial displacement was continuously recorded during the tests to evaluate the structural behavior of the specimens as a function of fire exposure duration and applied load level. Positive axial displacement was defined as column shortening under compression, whereas negative displacement represented axial elongation relative to the initial measurement position. The axial contraction limit of 30 mm and contraction-rate criterion of 9 mm/min were considered separately in evaluating the load-bearing response of the specimens. The recorded axial displacement was used to evaluate the deformation response of the specimens during fire exposure. The interpretation of the displacement measurements requires consideration of the measurement reference, sign convention, and potential contributions from loading-system movement and thermal expansion.

For specimen GL-C-L-1.2-1, subjected to a prescribed load ratio of 1.2, the target load of 370 kN could not be maintained consistently throughout the test. Therefore, although this specimen was included in the overall test program, it was excluded from subsequent quantitative comparisons of charring characteristics and axial displacement among different load ratios. The inability to maintain the prescribed target load was considered a limitation in the interpretation of this test condition, and no quantitative conclusions were drawn from this specimen regarding the relationship between applied load level and structural deformation.

2.4. Temperature Measurement

Thermocouples were installed within the GLT column specimens to monitor changes in internal temperature across the cross-section during fire exposure. The thermocouples were positioned at the mid-height of the specimens and arranged at different depths from the heated surface to measure the temperature distribution within the cross-section. For the specimens subjected to 180 min of fire exposure, the first thermocouple (CH1) was installed at a depth of 10 mm from the heated surface. Additional thermocouples were positioned at 5 mm intervals toward the interior of the cross-section, resulting in a total of 15 measurement channels, with the final thermocouple (CH15) located at a depth of 80 mm from the heated surface. For specimens subjected to fire exposure durations shorter than

180 min, the installation depths and number of thermocouples were adjusted according to the anticipated charring depth and fire exposure duration. A schematic illustration of the thermocouple locations and spacing from the heated surface is presented in Figure 4.

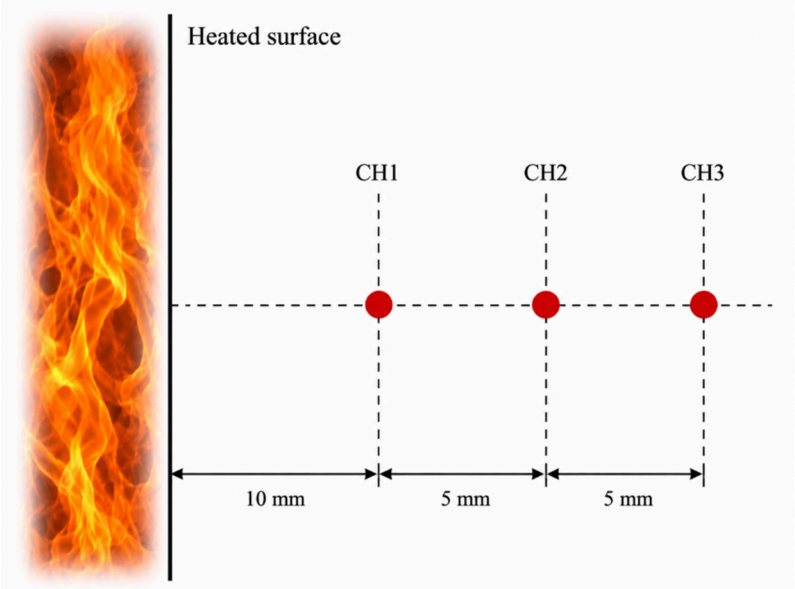


Figure 4. Schematic arrangement of thermocouples from the heated surface of the GLT column specimen.

Mineral-insulated metal-sheathed thermocouples with a diameter of 1.6 mm were used to measure the internal temperature of the GLT columns. Each thermocouple was connected to an external data logger, and changes in internal temperature were continuously recorded throughout the fire resistance test.

The thermocouples were installed at depths of 10–80 mm to monitor temperature changes at selected locations within the GLT cross-section during fire exposure, rather than to directly determine the final charring depth. This arrangement provided temperature measurements within the near-surface region during the progression of charring. However, because the final mean charring depths exceeded 100 mm after 180 min of fire exposure, the maximum instrumentation depth of 80 mm was insufficient to characterize the temperature distribution within the remaining uncharred section during the later stages of heating. Therefore, the thermal measurements were limited to the instrumented region, and the final charring depths were determined independently from post-test measurements, as described in Section 2.5.

2.5. Charring Depth Measurement

Charring depth was defined as the distance from the original surface of the specimen before fire exposure to the outer boundary of the residual cross-section after removal of the char layer following the fire resistance test. The final charring depth was determined from post-test measurements rather than from the thermocouple readings. At each designated measurement section, the char layer was removed to identify the boundary between the charred and remaining uncharred wood. The charring depth was then measured as the distance from the original specimen surface to this boundary. To account for variations in charring depth along the column height, four equally spaced measurement locations were established along the height of each specimen, and charring depth was measured at each corresponding cross-section. At each cross-section, charring depth was measured on all four faces of the column, resulting in a total of 16 charring depth measurements per specimen.

The 16 charring depth measurements obtained from each specimen were used to calculate a representative mean charring depth and were not treated as independent experimental replicates. Because only one specimen was tested under each experimental condition, the observed differences in charring characteristics may reflect both the investigated test variables and inherent material variability. Accordingly, the results were interpreted as comparisons between individual specimens rather than statistically established relationships. The locations of the measurement cross-sections along the column height and the charring depth measurement points at each cross-section are illustrated in Figure 5.

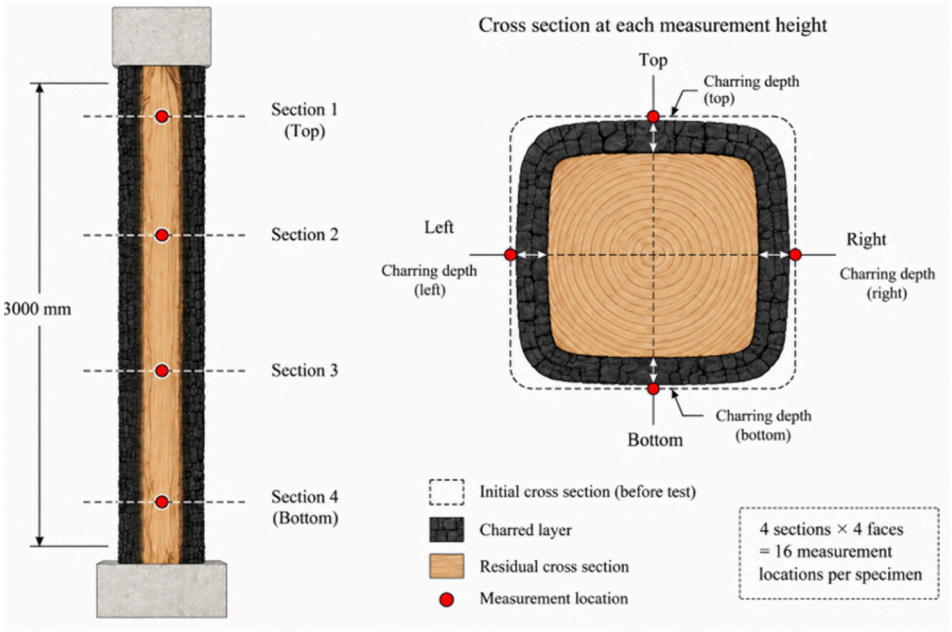


Figure 5. Charring depth measurement locations along the height and cross-section of the GLT column specimens.

The mean charring depth of each specimen was calculated using Equation (3).

$$d_{char,avg} = (\Sigma d_i)/n \quad (3)$$

where $d_{char,avg}$ represents the mean charring depth (mm), d_i denotes the charring depth measured at each measurement location (mm), and n is the total number of charring depth measurements, which was 16 in this study. The time-averaged charring rate (β_{avg}) of each specimen was calculated by dividing the mean charring depth by the corresponding fire exposure duration, as expressed in Equation (4). This value represents the cumulative average charring rate over the entire fire exposure duration rather than the instantaneous charring rate at a specific time.

$$\beta_{avg} = d_{char,avg}/\mathrm{t} \quad (4)$$

where β_{avg} represents the time-averaged charring rate (mm/min), $d_{char,avg}$ denotes the mean charring depth (mm), and t is the fire exposure duration (min). For the non-load-bearing tests, changes in charring behavior with increasing fire exposure duration were evaluated using the mean charring depths and time-averaged charring rates measured at 60, 90, 120, 150, and 180 min. In particular, the time-averaged charring rate calculated for each specimen was interpreted as an average over its entire fire exposure duration. For the load-bearing tests, the mean charring depths and time-averaged charring rates were determined for different load ratios under identical fire exposure conditions of 180 min. These results

were compared with those of the non-load-bearing specimen exposed to fire for 180 min to evaluate the influence of axial loading on the charring behavior of GLT columns.

To quantitatively evaluate the relationship between fire exposure duration and mean charring depth under non-load-bearing conditions, linear regression analysis was performed using the least-squares method. The analysis was based on the mean charring depths measured from specimens subjected to fire exposure durations of 60, 90, 120, 150, and 180 min. The slope and intercept of the linear regression equation were determined, and the goodness of fit of the regression model was evaluated using the coefficient of determination (R^2).

2.6. Residual Cross-Section Analysis

To quantitatively evaluate the reduction in cross-sectional area of GLT columns under fire exposure and examine its relationship with the axial deformation measured during the load-bearing tests, the residual cross-section was calculated using the mean charring depth measured after the fire resistance tests. The GLT columns investigated in this study had an initial square cross-section of 500 mm × 500 mm and were simultaneously exposed to fire on all four sides during testing. As fire exposure progressed, a char layer formed on the outer surfaces of the specimens. In this study, the residual cross-section was defined as the uncharred wood region remaining after excluding the char layer following the fire resistance test. The geometric residual cross-section includes both the heated but uncharred wood beneath the char layer and the relatively unaffected inner wood region. Therefore, it should be distinguished from the mechanically effective cross-section used in structural fire design, which additionally accounts for the reduction in mechanical properties caused by elevated temperatures. Figure 6 illustrates these regions to clarify the definition of the geometric residual cross-section adopted in this study. In Figure 6, c denotes the charring depth, b_0 represents the side length of the initial cross-section, and b_{res} represents the side length of the equivalent residual cross-section.

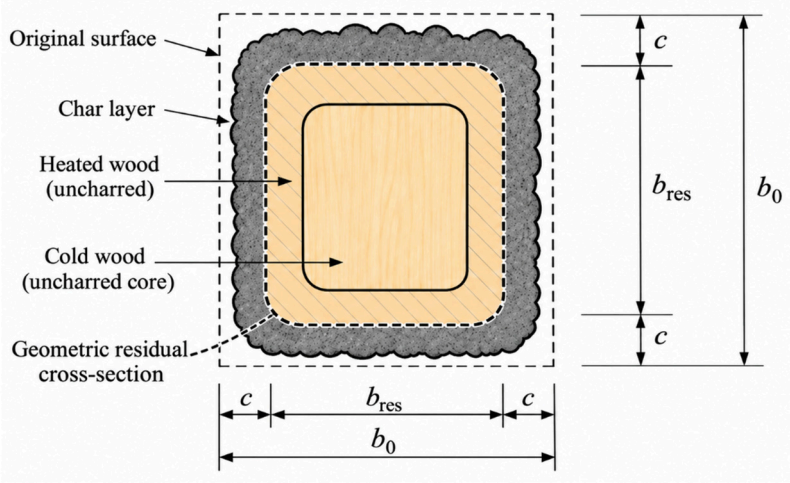


Figure 6. Schematic representation of the char layer, heated uncharred wood, and geometric residual cross-section of a GLT column under four-sided fire exposure.

The equivalent residual cross-section was calculated by assuming that the mean charring depth measured for each specimen occurred uniformly on all four exposed faces. Accordingly, the residual cross-section determined in this study represents a geometrically simplified cross-section, in which the irregular cross-sectional geometry remaining after fire exposure was approximated as a square using the measured mean charring depth. This approximation assumes uniform charring on all four exposed faces and along the column

height, although local variations in charring depth may occur due to differences in heat exposure, corner effects, and material characteristics. Consequently, the equivalent residual cross-sectional area calculated from the mean charring depth does not account for the spatial variability of charring or the irregular geometry of the actual residual cross-section. As a result, the calculated residual cross-sectional area may overestimate or underestimate the actual remaining area, particularly when nonuniform charring and localized corner recession produce an irregular residual cross-sectional geometry. Therefore, the calculated area should be interpreted as a simplified geometric indicator rather than an exact representation of the remaining cross-sectional area or the mechanically effective section used in structural fire design. A schematic illustration of char layer formation and the residual cross-section under four-sided fire exposure is presented in Figure 6.

The residual cross-section defined in this study excludes only the char layer and is therefore distinguished from the effective cross-section used in structural fire design, which additionally accounts for the region in which mechanical properties have deteriorated due to elevated temperatures [6,7]. Accordingly, the residual cross-section analysis was not intended to directly estimate the actual residual load-bearing capacity after fire exposure using a design-effective cross-section, but rather to examine the relationship between the geometric reduction in cross-sectional area with increasing fire exposure duration and the structural response observed during the load-bearing tests. Let b_0 denote the side length of the initial cross-section and $d_{char,avg}$ represent the mean charring depth of the specimen. The side length of the equivalent residual cross-section after fire exposure, b_{res}, was calculated using Equation (5).

$$b_{res} = b_0 - 2d_{char,avg} \tag{5}$$

Since the side length of the initial cross-section was 500 mm in this study, Equation (5) can be rewritten as Equation (6).

$$b_{res} = 500 - 2d_{char,avg} \tag{6}$$

The corresponding residual cross-sectional area, A_{res}, was calculated using Equation (7).

$$A_{res} = (500 - 2d_{char,avg})^2 \tag{7}$$

The initial cross-sectional area, A_0, is expressed in Equation (8).

$$A_0 = 500\,\text{mm} \times 500\,\text{mm} = 250,000\,\text{mm}^2 \tag{8}$$

To compare the extent of cross-sectional reduction at different fire exposure durations, the residual cross-sectional area ratio (R_A) was defined using Equation (9).

$$R_A = A_{res}/A_0 \tag{9}$$

The residual cross-sectional area ratio (R_A) represents the ratio of the residual cross-sectional area after fire exposure to the initial cross-sectional area. A value approaching 1.0 indicates that a greater proportion of the initial cross-section is retained. Conversely, the residual cross-sectional area ratio decreases as fire exposure duration and charring depth increase. To further examine the geometric implications of charring for column stability, the second moment of area of the equivalent square residual cross-section was calculated as $I_{res} = {b_{res}}^4/12$. The corresponding ratio to the initial second moment of area was expressed as $RI = (b_{res}/b_0)^4$. In addition, the radius of gyration was calculated as $r_{res} = b_{res}/\sqrt{12}$, allowing changes in the geometric slenderness parameter to be evaluated. These calculations represent geometric indicators and do not account for temperature-dependent reductions in elastic modulus, actual end restraints, or nonuniform charring.

For the non-load-bearing tests, changes in residual cross-sectional area and residual cross-sectional area ratio with increasing fire exposure duration were evaluated using the mean charring depths measured at 60, 90, 120, 150, and 180 min. For the load-bearing tests, the equivalent residual cross-section was calculated for each load ratio using the mean charring depth measured after 180 min of fire exposure. These results were compared with the measured axial displacement to investigate the influence of applied load level on the structural response of GLT columns exhibiting similar degrees of charring.

3. Charring Characteristics and Structural Behavior of GLT Columns Under Prolonged Fire Exposure

3.1. Effect of Fire Exposure Duration on the Charring Characteristics of GLT Columns

To evaluate the charring behavior of GLT columns as a function of fire exposure duration under non-load-bearing conditions, the results of standard fire resistance tests conducted at 60, 90, 120, 150, and 180 min were compared. The mean charring depth and time-averaged charring rate of each specimen were calculated using the methods described in Section 2.5. The measured mean charring depths at different fire exposure durations are presented in Figure 7.

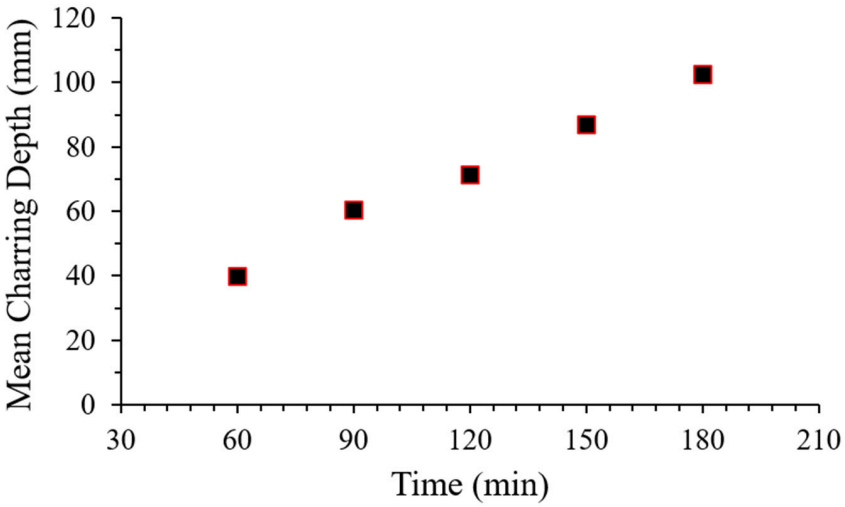


Figure 7. Measured mean charring depths of GLT columns at different fire exposure durations under non-load-bearing conditions.

The mean charring depths of the non-load-bearing specimens were 39.9, 60.4, 71.3, 86.8, and 102.6 mm at fire exposure durations of 60, 90, 120, 150, and 180 min, respectively. As the fire exposure duration increased from 60 to 180 min, the mean charring depth increased by 62.7 mm, with the value at 180 min being approximately 2.57 times that at 60 min. These results indicate that charring of the GLT columns progressed with increasing standard fire exposure duration, resulting in a gradual reduction in the original cross-sectional area.

To quantitatively evaluate the relationship between fire exposure duration and mean charring depth, linear regression analysis was performed on the non-load-bearing test results using the least-squares method. The resulting relationship between fire exposure duration (t) and mean charring depth ($d_{char,avg}$) is expressed by Equation (10).

$$d_{char,avg} = 0.506t + 11.48 (R^2 = 0.993) \quad (10)$$

where $d_{char,avg}$ represents the mean charring depth (mm), and t denotes the fire exposure duration (min). The linear regression analysis yielded a coefficient of determination (R^2) of 0.993, indicating a strong linear correlation between mean charring depth and fire exposure

duration within the investigated range of 60–180 min. The slope of the regression equation was 0.506 mm/min, representing the rate of increase in mean charring depth with increasing fire exposure duration within this range. However, the slope of the regression equation should be distinguished from the cumulative time-averaged charring rate calculated from the beginning of the test to each specified fire exposure duration. Furthermore, the intercept of 11.48 mm is a statistical parameter describing the fitted linear relationship and does not represent the actual charring depth at the beginning of fire exposure.

Meanwhile, the time-averaged charring rate was 0.67 mm/min at both 60 and 90 min, decreasing to 0.59, 0.58, and 0.57 mm/min at 120, 150, and 180 min, respectively. A comparison between the specimens exposed to fire for 60 and 180 min indicated a reduction of approximately 14.3% in the time-averaged charring rate, calculated using the values of 0.665 and 0.570 mm/min derived from the reported mean charring depths before rounding the rates to two decimal places. This trend is consistent with the general charring behavior of wood, in which the char layer formed during fire exposure delays heat transfer to the underlying wood [3–5]. In particular, while the mean charring depth continued to increase with increasing fire exposure duration, the cumulative time-averaged charring rate exhibited a decreasing trend.

However, the time-averaged charring rate calculated in this study represents the cumulative average over the entire fire exposure duration rather than the instantaneous charring rate at a specific time. Therefore, the observed reduction in time-averaged charring rate does not necessarily indicate a continuous decrease in the instantaneous charring rate throughout all exposure intervals. In fact, the increases in mean charring depth between successive 30 min exposure intervals were not uniform, suggesting possible variations in charring characteristics among the specimens. Furthermore, because only one specimen was tested at each fire exposure duration, the regression results have limitations in terms of their general applicability and should not be interpreted as a generalized predictive model for charring depth in all GLT columns.

Overall, the results demonstrate that the mean charring depth of large-section Korean larch GLT columns increased progressively under prolonged fire exposure, exhibiting a strong linear correlation with fire exposure duration within the investigated range of 60–180 min. In contrast, the cumulative time-averaged charring rate tended to decrease with increasing fire exposure duration. These findings provide fundamental experimental data for understanding the charring characteristics of large-section GLT columns subjected to prolonged fire exposure and for quantitatively evaluating the reduction in residual cross-sectional area as a function of fire exposure duration. The charring characteristics observed in this study were compared with those reported by Choi et al. [15], who investigated Korean larch GLT columns with a cross-section of 300 mm × 300 mm under standard fire exposure. In their non-load-bearing tests, mean charring depths of 40.5 and 77.1 mm were reported after 60 and 120 min, respectively. In comparison, the present study recorded mean charring depths of 39.9 and 71.3 mm at the corresponding exposure durations. Although the results are of a similar magnitude, differences in specimen dimensions and material characteristics prevent a direct attribution of these variations to cross-sectional size. Furthermore, the present study extends the investigation to 180 min, providing additional experimental observations of charring progression in larger GLT columns under prolonged standard fire exposure.

3.2. Comparison of Charring Behavior of GLT Columns Under Different Loading Conditions

To evaluate the influence of applied load on the charring behavior of GLT columns under prolonged fire exposure, the results of load-bearing and non-load-bearing fire resistance tests conducted for 180 min were compared. The load-bearing specimens subjected

to load ratios of 0.8 and 1.0 were included in the analysis, whereas the specimen with a load ratio of 1.2 was excluded from the quantitative comparison because the prescribed target load could not be consistently maintained during the test. The mean charring depth of the non-load-bearing specimen (GL-C-NL-3.0h-1) after 180 min of fire exposure was 102.6 mm. For the load-bearing specimens, mean charring depths of 106.5 and 107.3 mm were measured for GL-C-L-0.8-1 and GL-C-L-1.0-1, corresponding to load ratios of 0.8 and 1.0, respectively. These values were 3.9 and 4.7 mm greater than that of the non-load-bearing specimen, representing increases of approximately 3.8% and 4.6%, respectively. Furthermore, the difference in mean charring depth between the two load-bearing specimens was only 0.8 mm, indicating a relatively small variation despite the increase in load ratio from 0.8 to 1.0 under identical fire exposure conditions.

Figure 8 presents a comparison of the time-averaged charring rates of load-bearing and non-load-bearing specimens after 180 min of standard fire exposure. The time-averaged charring rate of the non-load-bearing specimen was 0.57 mm/min, whereas those of the load-bearing specimens with load ratios of 0.8 and 1.0 were 0.59 and 0.60 mm/min, respectively. Compared with the non-load-bearing specimen, the time-averaged charring rates of the load-bearing specimens were approximately 3.8% and 4.6% higher at load ratios of 0.8 and 1.0, respectively. However, the time-averaged charring rates of the two load-bearing specimens were similar, at 0.59 and 0.60 mm/min. These results indicate that relatively small differences in mean charring characteristics were observed between the load-bearing and non-load-bearing specimens under the investigated 180 min standard fire exposure conditions.

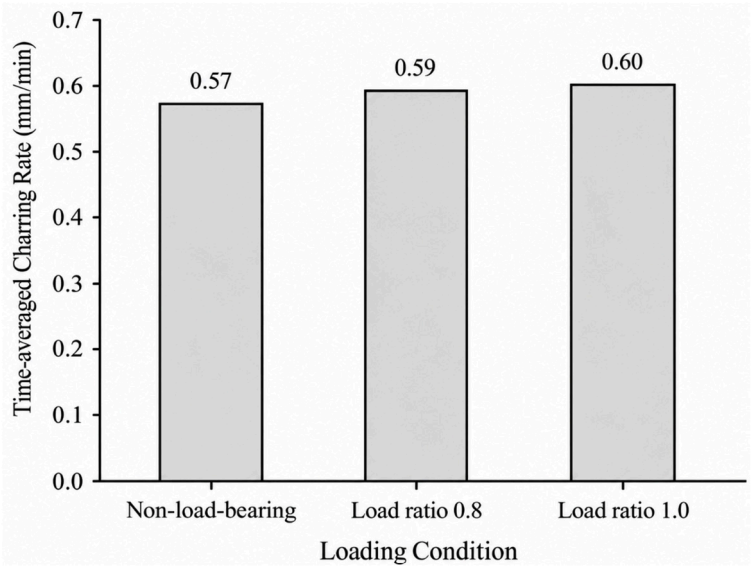


Figure 8. Comparison of time-averaged charring rates of GLT columns under non-load-bearing and different load-bearing conditions after 180 min of fire exposure.

Under identical fire exposure durations, the mean charring depths and time-averaged charring rates of the load-bearing specimens were slightly higher than those of the non-load-bearing specimen, although the differences were limited. In particular, the load-bearing specimens with load ratios of 0.8 and 1.0 exhibited similar mean charring depths and time-averaged charring rates, with relatively small differences observed between the two specimens under identical fire exposure conditions. These findings suggest that the structural response associated with different loading levels should be evaluated separately from charring characteristics when assessing the behavior of GLT columns under prolonged fire exposure.

However, because only one specimen was tested under each condition, the statistical significance of the observed differences in charring depth and charring rate could not be evaluated, and the results cannot establish a generalized relationship between applied load level and charring behavior. Therefore, the findings should not be interpreted as evidence that applied load has no influence on charring behavior. Rather, they indicate that the load-bearing and non-load-bearing specimens exhibited similar mean charring characteristics under the specific load ratios and fire exposure conditions investigated in this study. Previous experimental findings by Choi et al. [15] also reported relatively small differences in charring depth among Korean larch GLT column specimens subjected to load ratios of 0.9 or less. In the present study, the two load-bearing specimens exhibited similar mean charring depths of 106.5 and 107.3 mm after 180 min, despite having different prescribed load ratios. These observations provide additional experimental data on the charring characteristics of Korean larch GLT columns under prolonged fire exposure. However, differences in specimen dimensions, exposure durations, and experimental conditions, together with the absence of replicate tests, prevent a generalized conclusion regarding the influence of applied load on charring behavior.

3.3. Axial Deformation Behavior of GLT Columns Under Different Load Ratios

To evaluate the structural response of GLT columns under different load ratios during prolonged standard fire exposure for 180 min, the axial displacements of the load-bearing specimens were compared. Axial compressive loads of 247 and 309 kN were applied to the specimens with prescribed load ratios of 0.8 and 1.0, respectively. The axial displacement–time relationships of the specimens are presented in Figure 9.

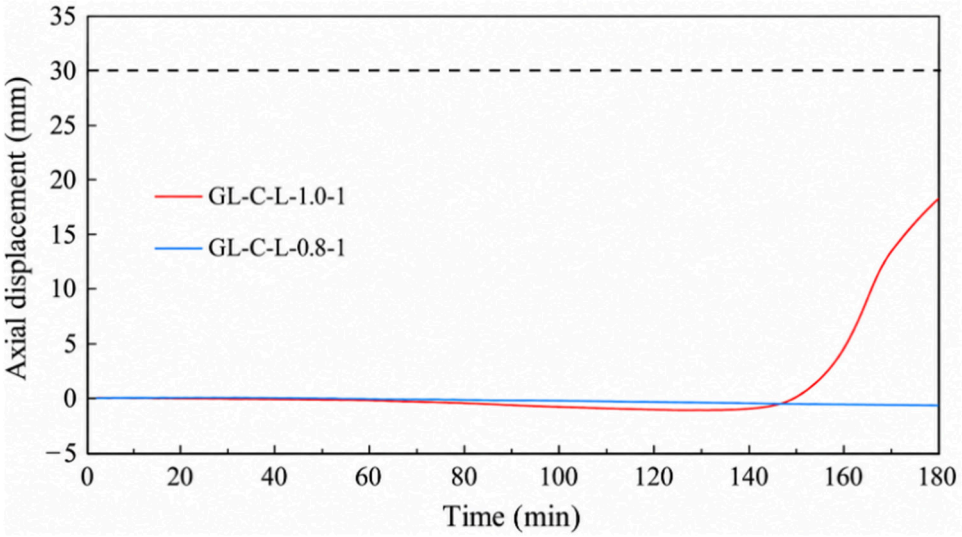


Figure 9. Axial displacement–time relationships of GLT columns subjected to different load ratios during 180 min of standard fire exposure. Positive and negative values indicate axial shortening and elongation, respectively.

The final axial displacement of specimen GL-C-L-0.8-1, subjected to a prescribed load ratio of 0.8, was −0.66 mm after 180 min of fire exposure, indicating a small net axial elongation relative to the initial measurement position. Relatively small variations in axial displacement were observed throughout the test. The negative displacement may reflect the combined effects of thermal expansion and compressive deformation; however, the individual contributions of these mechanisms could not be independently determined. In contrast, specimen GL-C-L-1.0-1 exhibited relatively small changes during the early and intermediate stages of fire exposure, followed by an increasing trend during the later

stage. A pronounced increase in axial displacement was observed after approximately 145 min, and the final displacement reached 18.35 mm at the end of the test, indicating axial shortening. The difference in final axial displacement between the two specimens was 19.01 mm. Although the specimen subjected to the higher applied load exhibited substantially greater axial deformation, the absence of replicate tests prevents this difference from being attributed exclusively to load level.

The pronounced increase in axial displacement observed after approximately 145 min may be associated with the combined effects of progressive cross-sectional reduction and temperature-dependent deterioration of wood mechanical properties. As charring progresses, the remaining cross-sectional area available to resist the applied compressive load decreases, while heating of the uncharred wood beneath the char layer may further reduce its strength and stiffness. These combined effects could contribute to increased compressive deformation during the later stages of fire exposure. However, although internal temperatures were monitored at selected depths during the tests, the temperature–time histories were not included in the present analysis. Therefore, a direct relationship between the onset of pronounced axial displacement and the internal temperature distribution could not be established. Furthermore, because the thermocouples were limited to depths of 10–80 mm, the temperature distribution within the remaining uncharred section could not be directly characterized during the later stages of fire exposure, preventing a quantitative evaluation of temperature-dependent reductions in elastic modulus and compressive strength. In addition, factors such as initial geometric imperfections, load eccentricity, and lateral deformation may have influenced the observed response. Accordingly, the deformation behavior should be interpreted as a specimen-specific observation rather than evidence of a particular temperature-dependent failure mechanism.

Previous investigations of laminated timber compression members have highlighted the importance of considering both cross-sectional degradation and structural stability when evaluating fire resistance [9]. In addition, Gernay et al. [13] investigated the structural response of timber columns during the cooling phase of fire exposure, demonstrating the importance of considering deformation and failure mechanisms beyond charring characteristics alone. Although the fire exposure conditions and investigated response stages differ from those of the present study, these findings provide context for interpreting the pronounced increase in axial displacement observed after approximately 145 min. The present results further illustrate that similar mean charring depths may be accompanied by substantially different axial deformation responses under prolonged standard fire exposure.

The dashed line in Figure 9 represents the axial contraction limit of 30 mm calculated for the specimen height of 3000 mm in accordance with KS F 2257-1. The final axial displacement of specimen GL-C-L-1.0-1 was 18.35 mm after 180 min, corresponding to approximately 61.2% of this limit. Although the contraction limit was not exceeded, the specimen exhibited a pronounced increase in axial displacement after approximately 145 min. The contraction-rate criterion of 9 mm/min represents a separate assessment parameter and should be evaluated using the axial displacement–time measurements. Therefore, the final displacement alone is insufficient to determine compliance with the contraction-rate criterion.

Overall, the two load-bearing specimens exhibited substantially different axial deformation responses despite having similar mean charring depths under identical fire exposure durations. These observations indicate the importance of considering both cross-sectional reduction and loading conditions when interpreting the structural fire behavior of large-section GLT columns. Nevertheless, additional replicated tests and measurements of lateral deformation and load eccentricity are required to establish the relative contributions of different deformation mechanisms.

3.4. Relationship Between Residual Cross-Sectional Area Reduction and Axial Deformation

To quantitatively evaluate the geometric reduction in the cross-sectional area of GLT columns as a function of fire exposure duration, the residual cross-section calculation method described in Section 2.6 was applied. Assuming that the mean charring depth of each specimen occurred uniformly on all four exposed faces, the residual cross-sectional area and residual cross-sectional area ratio were calculated based on the initial cross-sectional dimensions of 500 mm × 500 mm.

The calculated residual cross-sectional areas of the non-load-bearing specimens were 176,568, 143,793, 127,735, 106,537, and 86,907 mm^2 at fire exposure durations of 60, 90, 120, 150, and 180 min, respectively. The corresponding residual cross-sectional area ratios were 70.6%, 57.5%, 51.1%, 42.6%, and 34.8%, respectively. After 180 min of fire exposure, the residual cross-sectional area was calculated to have decreased by approximately 65.2% relative to the initial cross-sectional area.

These results demonstrate that the residual cross-sectional area of the GLT columns progressively decreased with increasing fire exposure duration. In particular, although charring depth increased approximately linearly with fire exposure duration, the residual cross-sectional area was calculated using a quadratic relationship involving charring depth. Consequently, a nonlinear geometric relationship exists between increasing charring depth and the reduction in cross-sectional area. The calculated second moment of area decreased more rapidly than the equivalent residual cross-sectional area as charring progressed. For the non-load-bearing specimens, the ratios of the residual to initial second moment of area were approximately 49.9%, 33.1%, 26.1%, 18.2%, and 12.1% at 60, 90, 120, 150, and 180 min, respectively. For the load-bearing specimens with load ratios of 0.8 and 1.0, the corresponding ratios after 180 min were approximately 10.9% and 10.6%, respectively. Furthermore, assuming an unchanged effective buckling length, the geometric slenderness ratios relative to the initial configuration increased to approximately 1.74 and 1.75 for the two load-bearing specimens. These results indicate that charring-induced cross-sectional reduction may substantially affect the flexural stiffness and geometric stability of GLT columns. However, the calculated values do not represent actual buckling capacities because temperature-dependent material degradation, end restraints, initial imperfections, and nonuniform charring were not explicitly considered. The variation in residual cross-sectional area ratio with fire exposure duration for the non-load-bearing specimens is presented in Figure 10.

Meanwhile, the residual cross-sectional areas of the load-bearing specimens after 180 min of fire exposure were calculated to be 82,369 and 81,453 mm^2 at load ratios of 0.8 and 1.0, respectively, corresponding to residual cross-sectional area ratios of approximately 32.9% and 32.6%. Although the difference in residual cross-sectional area between the two specimens was relatively small, at approximately 916 mm^2, their final axial displacements differed substantially, with values of −0.66 and 18.35 mm, respectively.

These results indicate that the structural response of GLT columns may vary depending on the applied load level, even when the geometric residual cross-sections calculated from the mean charring depths are similar. Specifically, the mean compressive stresses, calculated by dividing the applied loads by the final residual cross-sectional areas, were approximately 3.00 and 3.79 MPa for the specimens with load ratios of 0.8 and 1.0, respectively. This suggests that, under identical fire exposure conditions, differences in applied load may have a greater influence on the nominal compressive stress level than the relatively small differences in geometric residual cross-sectional area.

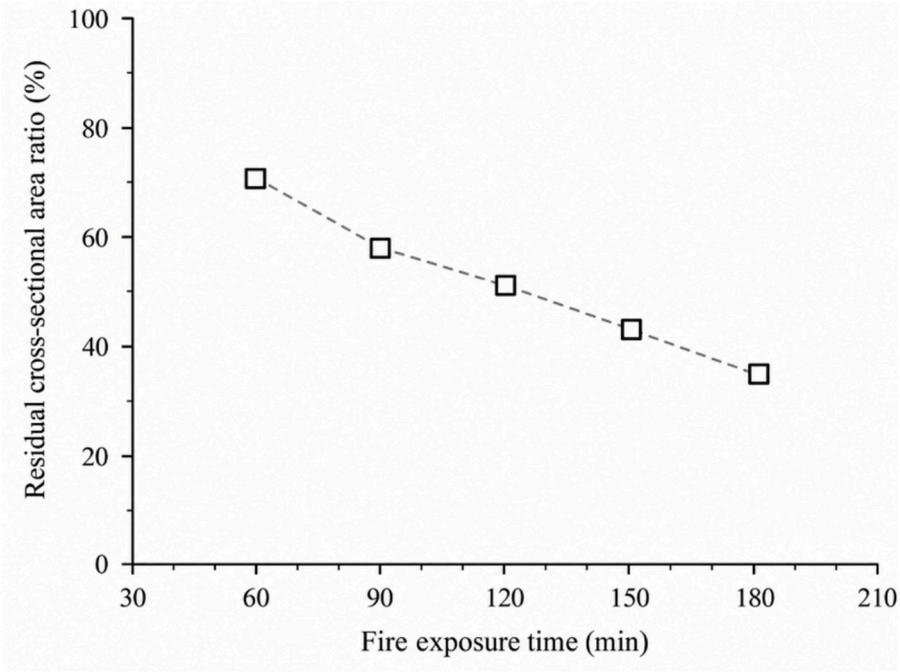


Figure 10. Variation in equivalent residual cross-sectional area ratio of non-load-bearing GLT columns with fire exposure duration.

From a mechanical perspective, the axial deformation of a GLT column under sustained compressive loading is influenced by the applied load, the remaining cross-sectional area, and the mechanical properties of the heated wood. As charring progresses, the reduction in the residual cross-sectional area increases the nominal compressive stress for a given axial load. At the same time, elevated temperatures may reduce the elastic modulus and compressive strength of the remaining uncharred wood, resulting in a reduction in axial stiffness. Furthermore, time-dependent deformation, including high-temperature creep under sustained loading, may contribute to the accumulation of axial displacement during prolonged fire exposure. In the present study, the specimen with a load ratio of 1.0 exhibited a higher nominal compressive stress than that with a load ratio of 0.8, despite their similar equivalent residual cross-sectional areas. These factors provide plausible mechanical explanations for the different axial deformation responses observed between the two specimens. However, temperature-dependent elastic moduli, creep strains, and the actual stress distributions within the residual cross-sections were not independently measured or quantified. Therefore, the individual contributions of these mechanisms to the observed displacement difference could not be established.

However, these mean compressive stresses are simplified values calculated using the applied loads and residual cross-sectional areas determined from the charring depths measured after the tests. Therefore, they do not directly represent the actual stress distribution within the cross-section during fire exposure or the structural load-bearing capacity of the specimens. Furthermore, the residual cross-section defined in this study represents the geometric cross-section remaining after excluding the char layer. It is distinguished from the effective cross-section used in structural fire design, which additionally accounts for the region beneath the char layer where the mechanical properties of wood have deteriorated due to elevated temperatures [6,7]. Furthermore, differences in local charring distribution and irregularities in the actual residual cross-sectional geometry may have influenced the axial deformation responses of the two load-bearing specimens, even though their equivalent residual cross-sectional areas were similar. Because these geometric variations were not independently quantified, their contributions to the observed displacement difference could

not be determined. Recent research by Zhang et al. [23] has further emphasized the importance of accounting for corner effects and residual cross-sectional geometry when assessing the post-fire load-carrying capacity of glulam columns. Their findings highlight the limitations of simplified cross-sectional assumptions in structural capacity assessment. In the present study, the equivalent residual cross-sectional area was used as a geometric indicator to compare the investigated specimens rather than to predict their residual load-bearing capacity. Accordingly, further investigations incorporating detailed residual cross-sectional geometry and temperature-dependent mechanical properties are needed to establish a more comprehensive relationship between charring progression and structural deformation.

Therefore, the residual cross-sectional area ratio presented in this study should be regarded as a geometric parameter for comparing the extent of cross-sectional reduction with increasing fire exposure duration and interpreting the axial deformation behavior under different load ratios, rather than as a design parameter for directly evaluating the actual residual compressive strength.

In comparison, the reduced cross-section method specified in Eurocode 5 [6] accounts for both the char layer and an additional zero-strength layer representing the loss of mechanical resistance in heated wood beneath the char layer. Therefore, the mechanically effective cross-sectional area used in structural fire design is generally smaller than the geometric residual area calculated in this study. However, the present analysis was limited to geometric cross-sectional reduction, and the temperature-dependent loss of mechanical properties was not quantified. Accordingly, the calculated residual areas should not be directly interpreted as effective load-bearing areas or used to predict the residual compressive capacity of the tested columns.

The thermal performance of adhesive bond lines may also influence the structural response of GLT columns during prolonged fire exposure. Elevated temperatures can affect adhesive bond integrity, potentially contributing to localized delamination and changes in charring or deformation behavior. However, the adhesive type and its temperature-dependent properties were not verified in the present study, and delamination was not independently evaluated. Therefore, the potential contribution of adhesive degradation or delamination to the observed structural response could not be determined. Further investigations incorporating verified adhesive properties and direct observations of bond-line behavior are required to clarify these effects.

Overall, this study quantitatively demonstrated the progressive increase in charring depth and reduction in residual cross-sectional area of large-section Korean larch GLT columns subjected to prolonged fire exposure. Furthermore, differences in axial deformation behavior were observed depending on the applied load level, even among specimens exhibiting similar residual cross-sectional areas under identical 180 min fire exposure conditions. These findings suggest that both charring-induced cross-sectional reduction and applied load level should be considered when evaluating the structural response of GLT columns subjected to prolonged fire exposure.

4. Conclusions

In this study, standard fire resistance tests were conducted on large-section glued-laminated timber (GLT) columns manufactured from Korean larch, with cross-sectional dimensions of 500 mm × 500 mm and a height of 3000 mm, for fire exposure durations of up to 180 min. To evaluate charring characteristics as a function of fire exposure duration, non-load-bearing fire resistance tests were performed at different exposure durations. Under load-bearing conditions, charring behavior and axial deformation were compared at different load ratios. Furthermore, changes in residual cross-sectional area were calculated based on the measured mean charring depths and examined in relation to the axial defor-

mation of the load-bearing specimens to evaluate the structural response of GLT columns under prolonged fire exposure. The main conclusions are summarized as follows.

1. Under non-load-bearing conditions, the mean charring depth of the GLT columns increased from 39.9 mm at 60 min to 102.6 mm at 180 min, whereas the time-averaged charring rate decreased from 0.67 to 0.57 mm/min. Linear regression analysis of the relationship between fire exposure duration and mean charring depth yielded a coefficient of determination (R^2) of 0.993, indicating a strong linear correlation within the investigated exposure range of 60–180 min. These results demonstrate that mean charring depth progressively increased with prolonged fire exposure, while the cumulative time-averaged charring rate exhibited a decreasing trend.
2. Under identical standard fire exposure conditions of 180 min, the mean charring depth of the non-load-bearing specimen was 102.6 mm, whereas those of the load-bearing specimens with load ratios of 0.8 and 1.0 were 106.5 and 107.3 mm, respectively. The corresponding time-averaged charring rates were 0.57 mm/min for the non-load-bearing specimen and 0.59 and 0.60 mm/min for the load-bearing specimens with load ratios of 0.8 and 1.0, respectively. Relatively small differences in mean charring depth and time-averaged charring rate were observed among the investigated specimens under identical fire exposure conditions. However, because only one specimen was tested under each condition, these observations do not establish a general relationship between applied load level and charring characteristics.
3. A comparison of axial deformation behavior under different load ratios showed that the specimen with a load ratio of 0.8 exhibited a final axial displacement of −0.66 mm after 180 min of fire exposure. In contrast, the specimen with a load ratio of 1.0 exhibited increasing axial displacement during the later stage of fire exposure, reaching a final value of 18.35 mm. Although the difference in mean charring depth between the two specimens was only 0.8 mm, their final axial displacements differed by 19.01 mm. These observations indicate that substantially different axial deformation responses occurred between the two investigated specimens despite their similar mean charring depths. However, because only one specimen was tested under each loading condition, the observed difference cannot be attributed exclusively to the applied load level, and further replicated tests are required to establish a general relationship between loading conditions and axial deformation.
4. The equivalent residual cross-sectional areas calculated from the mean charring depths showed that the residual cross-sectional area ratio of the non-load-bearing specimens decreased from 70.6% at 60 min to 34.8% at 180 min. For the load-bearing specimens exposed to fire for 180 min, the residual cross-sectional area ratios were similar, at 32.9% and 32.6% for load ratios of 0.8 and 1.0, respectively, whereas substantial differences were observed in their axial deformation behavior. These findings suggest that both the geometric reduction in residual cross-sectional area and the applied load level should be considered when evaluating the structural response of GLT columns subjected to prolonged fire exposure.
5. This study provides experimental evidence on the relationship among charring characteristics, residual cross-sectional reduction, and axial deformation behavior of large-section Korean larch GLT columns subjected to standard fire exposure for up to 180 min. However, only one specimen was tested under each experimental condition, and the residual cross-section was geometrically simplified using the mean charring depth without directly accounting for the degradation of wood mechanical properties at elevated temperatures. Therefore, further experimental investigations involving repeated tests and a wider range of loading conditions are necessary to validate the structural behavior of GLT columns under prolonged fire exposure and to quantita-

tively evaluate the relationship between residual cross-sectional characteristics and load-bearing capacity.

Author Contributions: Conceptualization, Y.C. and J.A.; methodology, J.A. and Y.C.; validation, H.A., J.A. and Y.C.; formal analysis, H.A.; investigation, J.A.; resources, J.A. and Y.C.; data curation, H.A.; writing—original draft preparation, H.A.; writing—review and editing, J.A. and Y.C.; visualization, H.A.; supervision, Y.C.; project administration, Y.C.; funding acquisition, J.A. and Y.C. All authors have read and agreed to the published version of the manuscript.

Funding: This research was funded by the 2026 Building Materials Certification Project (Fire Resistance and Sound Insulation) grant number 20260039-001.

Data Availability Statement: The original contributions presented in this study are included in the article. Further inquiries can be directed to the corresponding author.

Acknowledgments: The authors gratefully acknowledge the support of the Korea Institute of Civil Engineering and Building Technology (KICT) in conducting this research.

Conflicts of Interest: The authors declare no conflicts of interest.

References

1. Hart, J.; D'Amico, B.; Pomponi, F. Whole-life embodied carbon in multistory buildings: Steel, concrete and timber structures. *J. Ind. Ecol.* **2021**, *25*, 403–418. [CrossRef]
2. Skullestad, J.L.; Bohne, R.A.; Lohne, J. High-rise timber buildings as a climate change mitigation measure—A comparative LCA of structural system alternatives. *Energy Procedia* **2016**, *96*, 112–123. [CrossRef]
3. White, R.H.; Nordheim, E.V. Charring rate of wood for ASTM E 119 exposure. *Fire Technol.* **1992**, *28*, 5–30. [CrossRef]
4. Frangi, A.; Fontana, M. Charring rates and temperature profiles of wood sections. *Fire Mater.* **2003**, *27*, 91–102. [CrossRef]
5. Friquin, K.L. Material properties and external factors influencing the charring rate of solid wood and glue-laminated timber. *Fire Mater.* **2011**, *35*, 303–327. [CrossRef]
6. *EN 1995-1-2:2004*; Eurocode 5: Design of Timber Structures—Part 1-2: General—Structural Fire Design. CEN: Brussels, Belgium, 2004.
7. Schmid, J.; König, J.; Just, A. The reduced cross-section method for the design of timber structures exposed to fire—Background, limitations and new developments. *Struct. Eng. Int.* **2012**, *22*, 514–522. [CrossRef]
8. Schmid, J.; Klippel, M.; Just, A.; Frangi, A. Review and analysis of fire resistance tests of timber members in bending, tension and compression with respect to the reduced cross-section method. *Fire Saf. J.* **2014**, *68*, 81–99. [CrossRef]
9. Wiesner, F.; Bisby, L. The structural capacity of laminated timber compression elements in fire: A meta-analysis. *Fire Saf. J.* **2019**, *107*, 114–125. [CrossRef]
10. Ferreira, D.M.; Araújo, A.; Fonseca, E.M.M.; Piloto, P.A.G.; Pinto, J. Behaviour of non-loadbearing tabique wall subjected to fire—Experimental and numerical analysis. *J. Build. Eng.* **2017**, *9*, 164–176. [CrossRef]
11. Couto, D.L.P.; Fonseca, E.M.M.; Piloto, P.A.G.; Meireles, J.M.; Barreira, L.M.S.; Ferreira, D.R.S.M. Perforated cellular wooden slabs under fire: Numerical and experimental approaches. *J. Build. Eng.* **2016**, *8*, 218–224. [CrossRef]
12. Ali, F.; Kavanagh, S. Fire resistance of timber columns. *J. Inst. Wood Sci.* **2005**, *17A*, 85–93. [CrossRef]
13. Gernay, T.; Zehfuß, J.; Brunkhorst, S.; Robert, F.; Bamonte, P.; McNamee, R.; Mohaine, S.; Franssen, J.-M. Experimental investigation of structural failure during the cooling phase of a fire: Timber columns. *Fire Mater.* **2023**, *47*, 445–460. [CrossRef]
14. Li, X.; Kong, Y.; Zhu, L.; Lv, C.; Wu, J.; Wu, P.; Li, Q.; Xu, C.; Sun, K. Relationships between wood properties and fire performance of glulam columns made from six wood species commonly used in China. *Case Stud. Therm. Eng.* **2024**, *54*, 104029. [CrossRef]
15. Choi, Y.; Baik, K.; Kim, S.; An, J. A study on the charring properties of glued laminated Korean larch timber columns. *Sustainability* **2024**, *16*, 9130. [CrossRef]
16. Seyedrazavi, S.; Viau, C. Post-fire structural performance of glued-laminated timber columns subjected to real fires. *Structures* **2025**, *75*, 108772. [CrossRef]
17. Zheng, X.; Li, G.-Q.; Du, Y.; Lou, G. Experimental study on the charring behavior of glued laminated timber under large-space fire scenarios. *Fire Saf. J.* **2026**, *160*, 104605. [CrossRef]
18. *KS F 2257-1*; Methods of Fire Resistance Test for Elements of Building Construction—General Requirements. Korean Standards Association: Seoul, Republic of Korea, 2019.
19. *KS F 2257-7*; Methods of Fire Resistance Test for Elements of Building Construction—Specific Requirements for Columns. Korean Standards Association: Seoul, Republic of Korea, 2019.

20. *ISO 834-1:1999*; Fire-Resistance Tests—Elements of Building Construction—Part 1: General Requirements. ISO: Geneva, Switzerland, 1999.
21. *KDS 41 50 10:2022*; Timber Structures—Materials and Allowable Stresses. MOLIT: Sejong, Republic of Korea, 2022.
22. *KDS 41 50 20:2022*; Timber Structures—Design of Timber Structural Members. MOLIT: Sejong, Republic of Korea, 2022.
23. Zhang, Y.; Tan, M.; Li, H.; Yao, Y.; Wang, L.; Ni, W.; Zhang, X. Research on residual load-carrying capacity assessment and code applicability of glulam columns after fire exposure. *Constr. Build. Mater.* **2026**, *525*, 146395. [CrossRef]

Disclaimer/Publisher's Note: The statements, opinions and data contained in all publications are solely those of the individual author(s) and contributor(s) and not of MDPI and/or the editor(s). MDPI and/or the editor(s) disclaim responsibility for any injury to people or property resulting from any ideas, methods, instructions or products referred to in the content.